

# The Circadian Clock Gates the Intestinal Stem Cell Regenerative State

Phillip Karpowicz,<sup>1,\*</sup> Yong Zhang,<sup>2</sup> John B. Hogenesch,<sup>4</sup> Patrick Emery,<sup>2</sup> and Norbert Perrimon<sup>1,3,\*</sup>

<sup>1</sup>Department of Genetics, Harvard Medical School, Boston, MA 02115, USA

<sup>2</sup>Department of Neurobiology, University of Massachusetts Medical School, Worcester, MA 01605, USA

<sup>3</sup>Howard Hughes Medical Institute, Chevy Chase, MD 20815, USA

<sup>4</sup>Department of Pharmacology, University of Pennsylvania School of Medicine, Philadelphia, PA 19104, USA

\*Correspondence: [pkarpowicz@genetics.med.harvard.edu](mailto:pkarpowicz@genetics.med.harvard.edu) (P.K.), [perrimon@receptor.med.harvard.edu](mailto:perrimon@receptor.med.harvard.edu) (N.P.)

<http://dx.doi.org/10.1016/j.celrep.2013.03.016>

## SUMMARY

The intestine has evolved under constant environmental stresses, because an animal may ingest harmful pathogens or chemicals at any time during its lifespan. Following damage, intestinal stem cells (ISCs) regenerate the intestine by proliferating to replace dying cells. ISCs from diverse animals are remarkably similar, and the Wnt, Notch, and Hippo signaling pathways, important regulators of mammalian ISCs, are conserved from flies to humans. Unexpectedly, we identified the transcription factor *period*, a component of the circadian clock, to be critical for regeneration, which itself follows a circadian rhythm. We discovered hundreds of transcripts that are regulated by the clock during intestinal regeneration, including components of stress response and regeneration pathways. Disruption of clock components leads to arrhythmic ISC divisions, revealing their underappreciated role in the healing process.

## INTRODUCTION

Although many pathways that are required for healing have been discovered, little is known about how or whether healing is synchronized with general processes that regulate an animal's homeostasis and behavior. The circadian clock is an ancient molecular pathway that synchronizes organisms with daily environmental cues (zeitgebers) such as light intensity and temperature oscillations (Borgs et al., 2009; Hardin, 2011). Circadian rhythms are repeated over a 24 hr cycle, yet this chronological aspect of cell state has received little attention in the field of regenerative biology. For instance, many of the pathways that regulate intestinal regeneration and intestinal stem cells (ISCs) have been the subject of important studies (Biteau et al., 2011; Casali and Battle, 2009), but most of these studies did not consider whether results obtained during one part of the day occur at all times.

Circadian rhythms are thought to influence the cell cycle (Borgs et al., 2009), and there is some evidence that the clock plays a role in regeneration and proliferation. Hepatocyte cell division exhibits rhythms and is delayed following hepatectomy if circadian rhythms are disrupted (Matsuo et al., 2003). Earlier

studies in the intestine indeed found a daily rhythmicity in cell number and villus length (Qiu et al., 1994; Stevenson et al., 1979), as well as proliferation (Al-Nafussi and Wright, 1982; Potten et al., 1977), although clock mutants were not examined and ISCs were not specifically identified in those reports. Further, it was reported that metabolic processes display time-of-day variation in the intestine (Pan and Hussain, 2009; Saito et al., 1976; Scheving, 2000), and *per* mutation hastens tumorigenesis in Wnt pathway-driven colorectal cancer in mice (Wood et al., 2008). Finally, the degree of intestinal mucositis displays time-of-day variability in cancer patients treated by radiation (Shukla et al., 2010). This suggests that circadian rhythms may influence the intestine's regenerative response, although the reasons for this remain a mystery.

## RESULTS

### The *Drosophila* Intestine Has a Circadian Clock

The intestinal biology of *Drosophila* parallels that of mammals (Biteau et al., 2011; Casali and Battle, 2009) and allows for functional in vivo analyses to elucidate regenerative processes. *Drosophila* ISCs divide to produce progenitors called enteroblasts (EBs) that differentiate directly into absorptive enterocytes (ECs) or secretory enteroendocrine cells (Figure 1A). We performed a transgenic RNAi screen for transcription factors required in *Drosophila* ISCs during regeneration (see Experimental Procedures). It was previously shown that after damage occurs, ISCs regenerate the intestine by proliferating to replace dying cells (Biteau et al., 2011; Medema and Vermeulen, 2011). Here we discovered that among the ~600 genes tested, *period* (*per*) was required for proliferation of adult ISCs following damage by dextran-sodium sulfate (DSS), a chemical that models inflammatory bowel diseases in flies and mice (Amchevsky et al., 2009).

The *Drosophila* circadian pacemaker comprises the transcription factor partners *clock* (*clk*) and *cycle* (*cyc*), which are negatively regulated by *per* and *timeless* (*tim*; Hardin, 2011). One transcriptional target of CLK/CYC is *per* itself, which represses its own production and causes the cyclical transcriptional rhythms that underlie circadian rhythms. The existence of independent clocks throughout *Drosophila* tissues is known (Plautz et al., 1997), and we confirmed the cyclical accumulation and loss of *per* in the intestine when flies were kept on a 12 hr light/12 hr dark (LD) regimen (all of the experiments described below were performed under LD and chemical damage unless

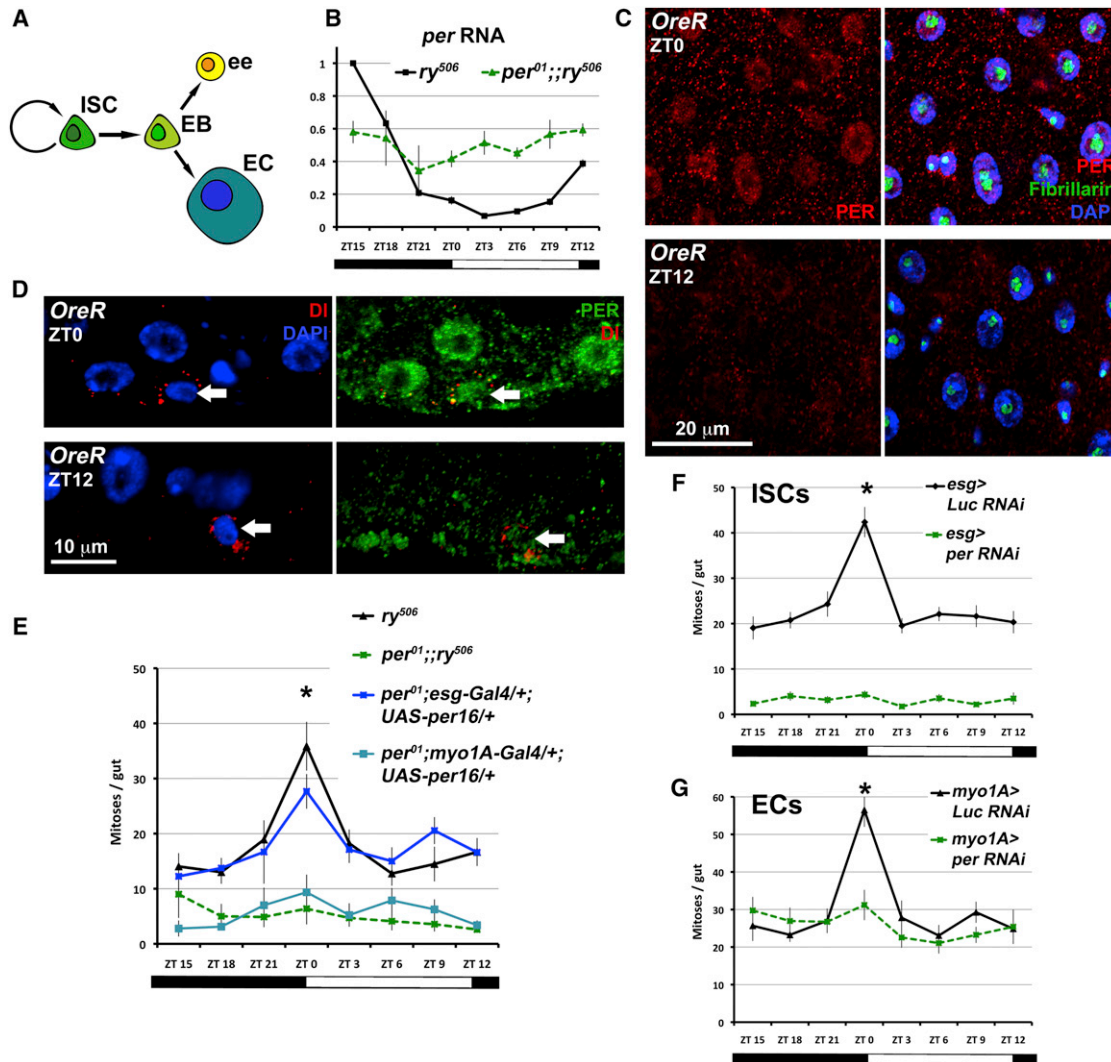


**Figure 1. PER Cycles and Functions in the Damaged Intestine**

(A) The ISC lineage. ISC, intestinal stem cell; EB, enteroblast; ee, enteroendocrine cell; EC, enterocyte.

(B) *per* RNA expression (qPCR) in the intestine over ZT, with ZT0 denoting when lights are turned on. The *ry*<sup>506</sup> control normally shows circadian rhythms, but these are absent in *per*<sup>01</sup> mutants. Graph shows the average of two separate experiments (n = 15 guts/genotype/time point, expression normalized to *ry*<sup>506</sup> ZT15, relative to *GAPDH* RNA; error bars ± SEM).

(C) PER staining (red) shows nuclear accumulation in intestinal cells in the morning (ZT0) versus the evening (ZT12). Fibrillarlin (green) marks the nucleolus, where PER is weaker.

(D) PER protein levels are rhythmic in ISCs (arrows) labeled with Delta (DI, red).

(E) When flies are maintained in LD conditions (see Figure S1C for schematic), control (*ry*<sup>506</sup>) intestinal mitoses peak at ZT0, in contrast to *per*<sup>01</sup>. A *UAS-per* rescue construct expressed in ISCs using *esg-Gal4* rescues this effect partially in the *per*<sup>01</sup> background.

(F) Rhythms are present in Luciferase (*esg > Luc RNAi* is *esg-Gal4/+; UAS-dcr2/UAS-Luc RNAi*) controls, but PER knockdown in ISCs (*esg > per RNAi* is *esg-Gal4/+; UAS-dcr2/UAS-per RNAi*) phenocopies *per*<sup>01</sup>.

(G) PER knockdown in ECs also disrupts circadian mitotic rhythms (genotypes as above but with *myo1A-Gal4/+*).

See also Figures S1, S2, S3, and S5.

otherwise noted). Quantitative RT-PCR (qRT-PCR) confirmed that *per* mRNA accumulates in the early evening (zeitgeber time 12–18 [ZT12–18]; Figures 1B and S1A), and staining for PER confirmed its nuclear accumulation in the late night/early morning (Figure 1C, ZT0). PER is expressed in the epithelial cells of this tissue (the polyploid ECs as well as the diploid ISCs; Figures 1D and S1).

### The Clock Gene *per* Regulates Rhythmic Intestinal Regeneration

The *per*<sup>01</sup> allele is a loss-of-function nonsense mutation (Hardin et al., 1990). Although they are viable, *per*<sup>01</sup> mutant animals do not exhibit circadian gene expression or behavioral rhythmicity (Figures 1B, S1, and S2). We assayed the regenerative response of *per*<sup>01</sup> ISCs following damage by DSS. Only the ISCs in the

*Drosophila* intestine divide (Ohlstein and Spradling, 2006), and mitotic ISCs were scored by phosphorylated histone H3 positivity. Control ( $ry^{506}$ ) ISCs show a peak in mitoses occurring at dawn (Figure 1E, ZT0), the transition between night and day when PER accumulates. This peak is absent in  $per^{01}$  intestines, which show reduced mitoses at all time points (Figure 1E). A *UAS-per* transgene, which restores circadian rhythms behaviorally when expressed in pacemaker neurons (Figure S2), partially restored the mitotic peak in  $per^{01}$  when expressed in ISCs using *esg-Gal4* (Amcheslavsky et al., 2009), but not in ECs using *myo1A-Gal4* (Jiang et al., 2009; Figure 1E). Importantly, the *esg-Gal4* and *myo1A-Gal4* drivers are not expressed in pacemaker neurons, and do not rescue  $per^{01}$  arrhythmic behavior when driving *UAS-per* (Figure S2). A characteristic of circadian rhythms is their free-running nature (Hardin, 2011), which we tested by shifting flies to constant darkness (DD) after LD entrainment. PER expression rhythms and intestinal mitotic rhythms perpetuate in DD, demonstrating their circadian nature (see Figures S1F and S5A–S5C). Together, these results show that ISCs divide according to a circadian rhythm in response to damage, and that this response is *per* dependent.

Undamaged  $per^{01}$  intestines do not show obvious deficiencies in epithelial cell types (Figures S3A and S3B) or rhythmic mitoses (see Figure 4C). Both ISCs and ECs participate in regeneration (Biteau et al., 2011), raising the question as to which cells are responsible for the inability of  $per^{01}$  intestines to display mitotic rhythms. A second important question is whether mitotic rhythms in response to damage are linked to behavioral activity or feeding (Xu et al., 2008). We validated a *UAS-per RNAi* construct for its ability to reduce PER expression and abolish circadian behavior rhythms (Figure S2). PER knockdown in ISCs phenocopied the arrhythmic  $per^{01}$  intestine (Figure 1F) and, strikingly, PER depletion in ECs also abolished ISC proliferation rhythms (Figure 1G). These phenotypes are not correlated with circadian behavior (Figure S2) or feeding (Figures S3C and S3D), which are rhythmic (although we do note an  $\sim 1$  hr circadian period lengthening in the *esg-Gal4* driver). Since only ISCs divide in this tissue, *per RNAi* disruption in ISCs (Figure 1F) accounts for the  $per^{01}$  phenotype (Figure 1E), whereas *per RNAi* in ECs simply abolishes a peak at ZT0 (Figure 1G). These results suggest that PER is required separately in both ISCs and ECs to produce intestinal mitotic rhythms, and that these rhythms are separate from feeding and behavioral rhythms.

Next, we generated *per*-deficient mutant clones to test whether the defect associated with PER loss was cell autonomous. Following damage,  $per^{01}$  and *per RNAi* clones are slightly smaller (Figure S4) and show reduced size over long periods of time in the absence of acute damage. This suggests that PER has a weaker ISC-autonomous role in initiating or boosting proliferation following damage or stress, but that overall a stronger nonautonomous role is predominant.

### The Core Clock Functions during Intestinal Regeneration

Because *per* and *tim* work together to inhibit *clk/cyc*, the outcomes of CYC activity would be expected to oppose those of PER. The  $cyc^0$  and  $tim^0$  loss-of-function mutants are also viable, and also display altered intestinal mitotic rhythms in response to

damage (Figures 2A and 2B). The expression of a *UAS-cyc* transgene in ISCs (*esg-Gal4*) in the  $cyc^0$  background was able to partially rescue this phenotype, but expression in ECs (*myo1A-Gal4*) did not (Figure 2A). Although the  $cyc^0$  phenotype is the opposite of the  $per^{01}$  phenotype, we note that the  $tim^0$  phenotype is not the same as that of  $per^{01}$ , suggesting that *tim* may have additional functions in this tissue. It is also possible that genetic background plays a role in the level of mitoses observed in these conditions. We tested the epistatic relationships between these genes. The  $per^{01};tim^0$  double mutant displays the  $per^{01}$  phenotype (Figure 2C), and the  $cyc^0;per^{01}$  double mutant displays the  $cyc^0$  phenotype (Figure 2D), as would be predicted from the circadian clock transcriptional feedback loop, which undergoes circadian rhythms in this tissue (Figure S1). We further tested the requirement of CYC in the regenerative process by expressing a functionally validated *UAS-cyc RNAi* construct (Figures S2 and S3) in ISCs and ECs. CYC is required in both of these cell types to produce mitotic rhythms, and the loss of CYC in either ISCs (Figure 2E) or ECs (Figure 2F) abolished any rhythms observed. Light levels entrain the circadian clock, and when flies are exposed to light-only (LL) conditions, the rhythmic nature of mitoses is abolished and remains constant at all time points (Figures S5E–S5G). Altogether, these data confirm that the circadian clock is required in both ISCs and their EC neighbors for mitotic rhythms.

Bleocin is a potent DNA-damaging chemical that causes apoptosis in the intestine (Amcheslavsky et al., 2009), and it was applied to investigate the outcome of a circadian-deficient damage response. Following Bleocin-induced damage, mitoses in control versus  $cyc^0$  and  $per^{01}$  mutant flies show phenotypes similar to those observed under DSS (Figure 2G). The  $cyc^0$  mutants exhibit reduced survival on Bleocin (Figure 2H) or DSS (Figure S5), and  $per^{01}$  and  $tim^0$  show similar reduced survival (Figures 2H, 2I, and S5). The knockdown of CYC or PER within ISCs or ECs results in reduced survival on Bleocin (Figures 2J and 2K). Hence, the disruption of the circadian clock either throughout the body or only in ISCs or ECs negatively impacts the survival of animals when the intestine is damaged.

### Clock-Deficient ISCs Lag in the Cell Cycle during Regeneration

The accumulation of mitotic  $cyc^0$  ISCs (Figure 2A) suggests that loss of *cyc* throughout the animal causes ISCs to overproliferate or stalls these cells in mitosis. An EdU uptake assay, which measures cells in S phase, revealed that control ( $ry^{506}$ ) ISCs show a peak in S phase at ZT6. The  $cyc^0$  and  $per^{01}$  mutants do not exhibit any peaks, and  $cyc^0$  mutants do not exhibit increased S phase (Figures 3A and 3B). Hence, it is unlikely that  $cyc^0$  ISCs overproliferate, and *cyc RNAi* clones also did not show an overproliferation phenotype (Figure S4).

We applied the FUCCI cell-cycle reporter (Nakajima et al., 2011; Sakaue-Sawano et al., 2008), which accumulates *mAG-Geminin* during S/G2/M phases (Azami Green positive), to determine cell-cycle states when circadian rhythms are absent in ISCs. We expressed the FUCCI reporter along with *cyc RNAi* or *per RNAi* with *esg-Gal4*, and identified ISCs using D1+. The control RNAi lines show a gradual accumulation of S/G2/M-phase-positive ISCs up to ZT18, when these cells divide

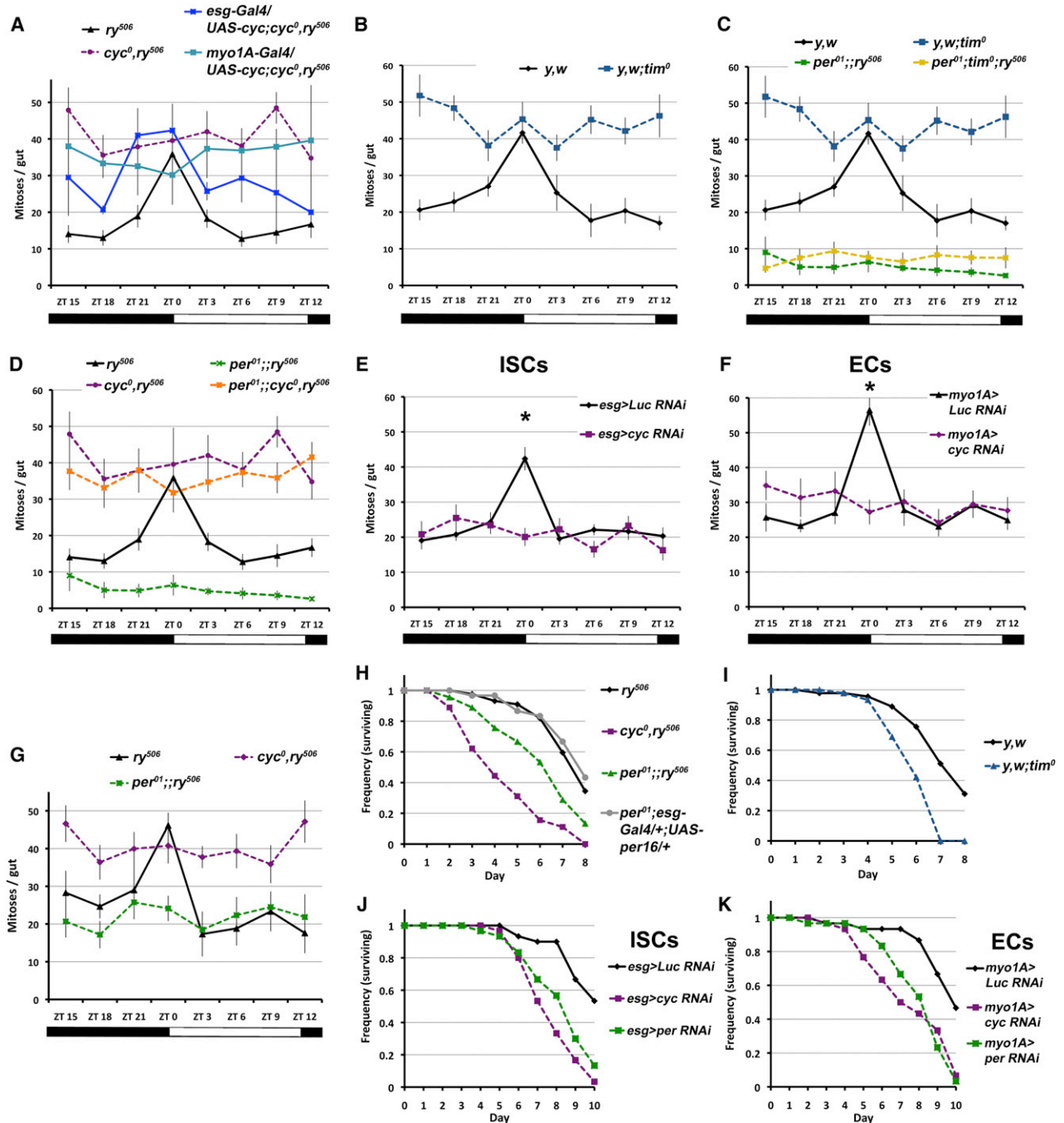


**Figure 2. The Circadian Clock Is Required in the Damaged Intestine**

(A and B) When flies are maintained in LD conditions, control (*ry<sup>506</sup>* and *y,w*) intestinal mitoses peak at ZT0, in contrast to *cyc<sup>0</sup>* and *tim<sup>0</sup>* mutants. A *UAS-cyc* construct expressed in ISCs (*esg-Gal4*) partially restores this rhythm in the *cyc<sup>0</sup>* background. *ry<sup>506</sup>* data are duplicated from Figure 1E.

(C and D) *per<sup>01</sup>;tim<sup>0</sup>* double-mutant intestines resemble the *per<sup>01</sup>* mutant phenotype. *per<sup>01</sup>;cyc<sup>0</sup>* double-mutant intestines resemble the *cyc<sup>0</sup>* mutant phenotype. Control and mutant data are duplicated from Figures 1E, 2A, and 2B.

(E and F) *CYC* knockdown in ISCs (*esg > cyc RNAi* is *esg-Gal4/+; UAS-dcr2/UAS-cyc RNAi*) or in ECs (*myo1A > cyc RNAi* is *myo1A-Gal4/+; UAS-dcr2/UAS-cyc RNAi*) disrupts circadian mitotic rhythms. Control data are from Figures 1F and 1G. All graphs show the average of two separate experiments ( $n = 10$  guts/genotype/time point, error bars  $\pm$  SEM, \* $p < 0.05$  at ZT0).

(G) Following Bleocin exposure, control (*ry<sup>506</sup>*) intestinal mitoses peak at ZT0, in contrast to *per<sup>01</sup>* and *cyc<sup>0</sup>*, similarly to what happens following DSS damage.

(H and K) The survival rates of all circadian clock mutants as well as animals in which PER or CYC was knocked down by RNAi in either ISCs or ECs are reduced compared with controls on Bleocin (black lines). Graphs show representative experiments ( $n = 3$  vials, 15 flies per vial; genotypes as above).

See also Figures S1, S2, S3, and S5.

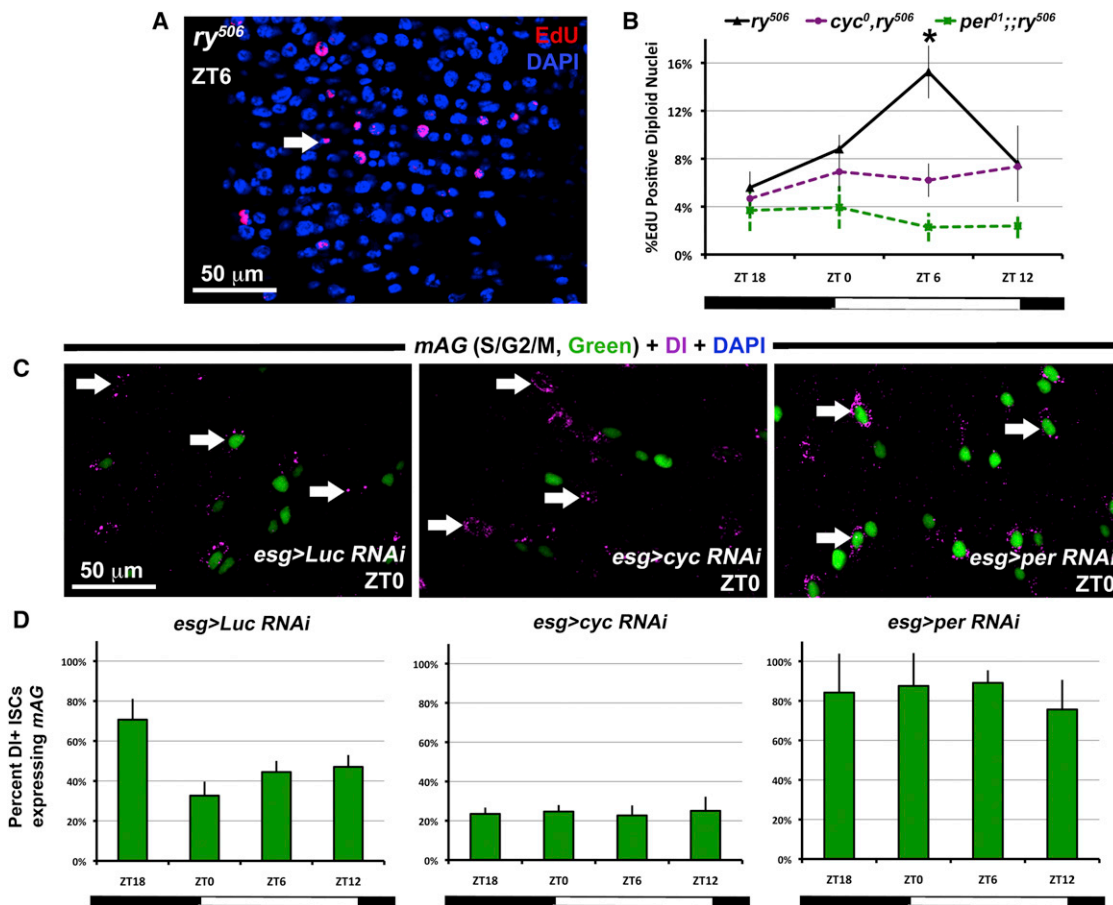


**Figure 3. Circadian Rhythms Synchronize Cell-Cycle Phases in ISCs**

(A and B) Dissected intestines of flies were exposed to the thymidine analog EdU for 45 min to detect S phase cells (red). Control ( $ry^{506}$ ) diploid cells in the intestine show a peak of S phase at ZT6, but neither  $cyc^0$  nor  $per^{01}$  shows this rhythm ( $n = 5$  guts/genotype/time point, error bars  $\pm$  SEM,  $*p < 0.05$  at ZT6).

(C) The intestines of the Fucci cell-cycle reporter: *mAG* marks cells in S/G2/M phases, and DI+ ISCs are indicated with arrows. Analysis is carried out in ISCs (for example, the control *esg > Luc RNAi* indicates *esg-Gal4 / UAS-S/G2/M-Green; UAS-Luciferase RNAi / +*).

(D) Quantification of DI+ ISCs suggests that most *esg > cyc RNAi* ISCs are negative at all time points, whereas *esg > per RNAi* are positive (green).

See also Figures S2 and S3.

(Figures 3C and 3D). However, not all ISCs are in S/G2/M phases, indicating that a significant reserve population of ISCs exists at all times. Irrespective of time, nearly all *cyc RNAi* ISCs are S/G2/M phase negative, whereas nearly all *per RNAi* ISCs are positive. Because its loss causes ISCs to accumulate in G1 (or G0), these results suggest that CYC promotes the G1 to S phase transition. Conversely, when PER is lost, movement through G1 is unopposed, but ISCs accumulate after S phase entry without entering mitosis (see Figure 1F). Thus, we propose that the circadian clock regulates the G1 to S phase transition in ISCs following damage.

### The Clock Regulates the Transcription of Hundreds of Genes in the Intestine

More than 10% of all mammalian genes are regulated in a circadian fashion (Panda et al., 2002), and components of the clock directly regulate transcription in a tissue-specific manner (Abruzzi et al., 2011; Akhtar et al., 2002), suggesting that a

tremendous variety of cell states are outcomes of circadian processes. Since *per* RNA and protein oscillate in the midgut, and *per* was identified in our screen, we performed genome-wide expression analysis on  $ry^{506}$  control intestines and  $cyc^0$  mutants over 24 hr following damage (Figure 4A; Tables S1, S2, and S3). We reasoned that clock target genes would show 24 hr rhythms and would be perturbed if CLK/CYC were disrupted. We found that 433 genes were rhythmic in controls, like *per*, but arrhythmic in  $cyc^0$ , indicating that they are under clock regulation in this tissue (Table S1). For instance, *Connector of kinase to AP-1 (Cka)*, a scaffold protein required for signal transduction of the JNK stress-response pathway (Chen et al., 2002), peaks at ZT15 (Figure 4B). Direct CLK/CYC targets would be expected to be strongly reduced in  $cyc^0$  mutants, yet only 21 of 433 genes (including *per* and *tim*) fit this profile (Table S2); hence, most rhythmic genes are likely to be indirectly regulated. Two hundred rhythmic genes showed the opposite phase to that of *per*, suggesting they are regulated by the transcription factors *vriille* or

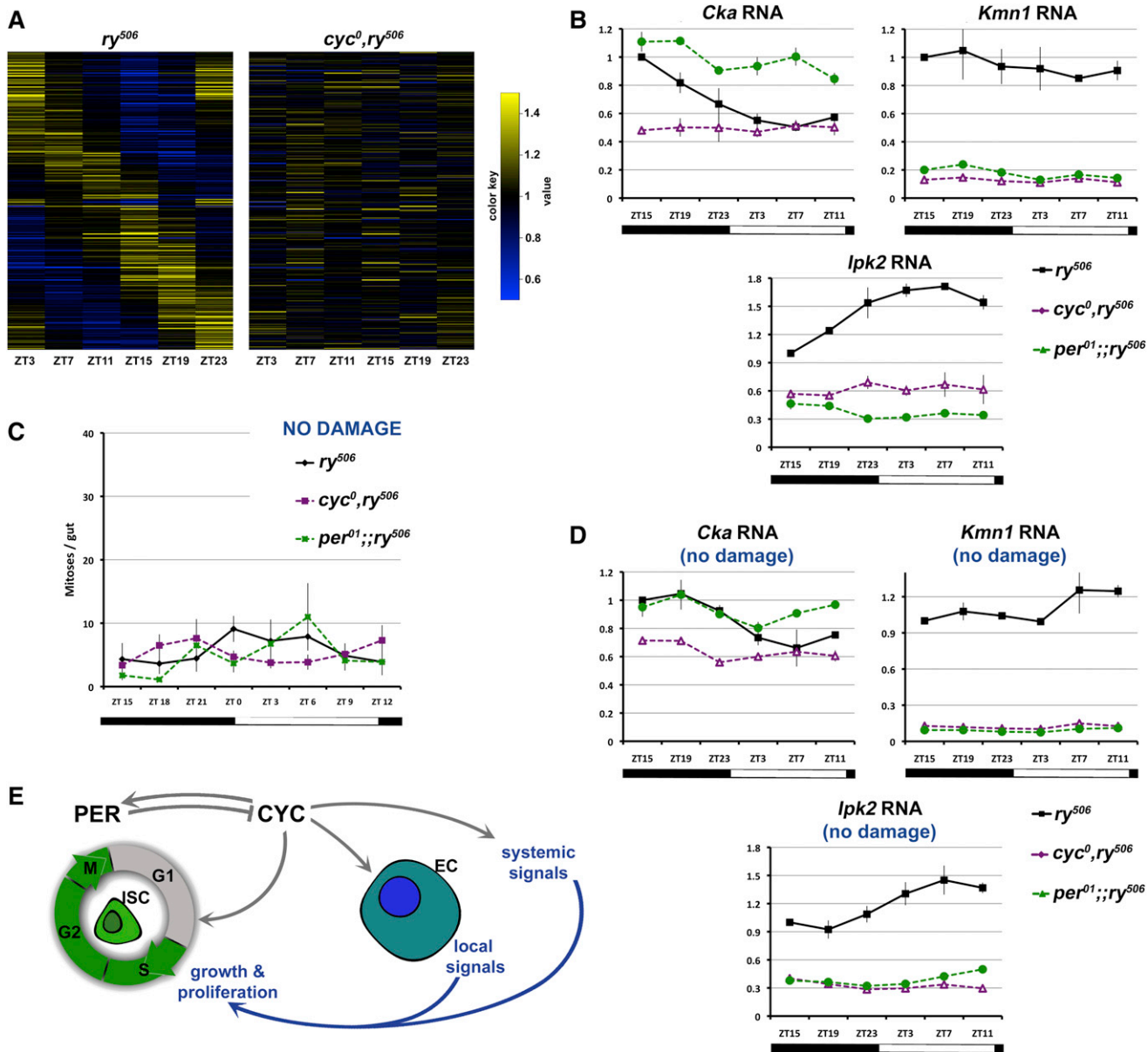


**Figure 4. The Clock Regulates the Expression of Diverse Transcripts**

(A) All genomic transcripts were interrogated for rhythmic expression during regeneration. Heat maps reveal 433 genes with circadian rhythms in *ry<sup>506</sup>* controls but not in *cyc<sup>0</sup>* mutants.

(B) *Cka*, *Ipk2*, and *Kmn1* RNA expression (qPCR) in the intestine over 24 hr. *Cka* shows *per*-like rhythms, whereas *Ipk2* exhibits antiphasic rhythms. *Kmn1* displays no circadian rhythmicity but is significantly downregulated in the *cyc<sup>0</sup>* mutant. Graphs are reported as in Figure 1B.

(C) Flies maintained in LD conditions on regular media do not show a mitotic peak at ZT0, in contrast to when the intestine is damaged. Under these conditions the mitotic index is similar between *ry<sup>506</sup>* controls and *cyc<sup>0</sup>* or *per<sup>01</sup>* mutants.

(D) In the absence of damage, the expression of *Cka* and *Ipk2* (qPCR) is rhythmic, similar to what is observed during regeneration. *Kmn1* (qPCR) also shows lower expression both before and after damage.

(E) A model of how the clock synchronizes ISC division: CYC is important for the transition through G1, and the clock also initiates systemic signals and local niche signals originating from ECs. Together, these signals activate ISC divisions, most likely through nonautonomous mechanisms.

See also Figures S2, S3, and S5.

*Pdp1*, which are part of the clock and together generate antiphasic transcript rhythms that peak in the early day (Hardin, 2011; Table S1). One of these, *Ipk2*, is an inositol phosphate kinase

and a positive regulator of Jak/STAT signaling (Müller et al., 2005), a pathway that is critical during intestinal regeneration (Figure 4B). Another one of these genes, *bazooka*, was recently

reported to polarize ISCs (Goulas et al., 2012), suggesting that the clock also regulates cell polarity. An additional 205 genes showed low expression in *cyc*<sup>0</sup> mutants but did not display rhythms (Table S3). This includes *Kmn1*, which enables chromosome segregation during anaphase (Venkei et al., 2011), suggesting that mitosis could be disrupted (Figure 4B). Overall, a great diversity of intestinal transcripts are thus influenced by the clock.

## DISCUSSION

Circadian pathway mutants are viable and their cells readily proliferate during development. Unlike other tissues (Abruzzi et al., 2011; Borgs et al., 2009), cell-cycle regulators do not seem to be clock targets in the intestine (Table S1). Although they are readily detected, neither cyclins nor regulators such as *Wee1* (Matsuo et al., 2003) exhibit circadian rhythms in this tissue. In the absence of acute damage, clock mutant ISCs divide normally (Figure 4C) and have no ISC-autonomous phenotypes (Figure S4). So it is quite surprising that PER and CYC are critical for adult ISC division during regeneration.

The ISC-autonomous phenotypes that occur during regeneration are modest compared with those that arise when the clock is disrupted systemically or in all ISCs/ECs by RNAi. This suggests that the clock predominantly regulates nonautonomous functions and may be involved in the synchronization of cell states across this tissue during the damage response. Indeed, because *esg-Gal4* is expressed in both ISCs and their immediate progeny (the EBs) for some time while they differentiate, it is possible that the clock regulates EB-to-ISC signaling. Intriguingly, disruption of the circadian clock in different cells leads to the accumulation of ISCs in different cell states; for instance, the *cyc*<sup>0</sup> mutant stalls during mitosis when CYC is absent systemically (Figure 2A), whereas it stalls during G1 if CYC is depleted in all ISCs (Figures 3C and 3D). This G1 lag explains why *cyc* RNAi ISCs show reduced mitoses compared with the *cyc*<sup>0</sup> mutant; however, given that the mechanisms underlying these processes are unresolved, it is possible that these differences are due to genetic background. At present, we thus conclude that rhythmic cell proliferation normally occurs in the damaged intestine and that this is dependent on the clock. We also note that forced expression of *per* or *cyc* in ISCs is able to partially restore rhythmic divisions in their respective mutant backgrounds (Figures 1E and 2A), whereas disruption of these genes in only ECs perturbs ISC rhythmic division (Figures 1G and 2F). This highlights the complexity of clock-regulated processes and suggests that desynchrony between ISCs and their surrounding cells (Figures S1G and S1H) can have different outcomes.

Circadian rhythms occur in many intertwined processes, including metabolism (Sahar and Sassone-Corsi, 2009), post-transcriptional regulation (Koike et al., 2012), and oxidation-reduction cycles (O'Neill and Reddy, 2011). The rhythmic expression of *Cka*, which brings together kinases and transcription factors to transduce JNK signal (Chen et al., 2002), and *lpk2*, which may boost the activity of cytokines involved in regeneration (Müller et al., 2005), suggests that the clock sensitizes the intestine to engage the regenerative response at specific times. For instance, several of the genes that exhibit circadian rhythms

during regeneration also show these rhythms prior to damage (Figure 4D). An emergent function of the clock could be to coordinate stem cell states according to either local niche signals or systemic signals, each of which would be under autonomous circadian control (Figure 4E).

Although *per* mutation increases cancer incidence (Borgs et al., 2009; Fu et al., 2002; Wood et al., 2008) and cancer cell proliferation (Borgs et al., 2009; Janich et al., 2011), our work suggests it is not simply a tumor suppressor. Recently, the circadian clock was shown to influence mammalian blood and hair stem cell biology (Janich et al., 2011; Méndez-Ferrer et al., 2008). In particular, hair stem cells are strikingly heterogeneous in their circadian rhythm activity (Janich et al., 2011), for unknown reasons. The coordination of proliferation, by synchronizing internal with external rhythms, may thus represent an important difference between normal stem cells and neoplastic cells.

## EXPERIMENTAL PROCEDURES

Animals were maintained at 25°C under LD conditions and damaged by being fed 5% w/v DSS (MP Biomedicals) or 25 µg/mL Bleocin (Calbiochem). The flies were maintained under LD conditions as before, except for experiments in which the light conditions were changed to complete darkness or complete light. Female flies < 14 days of age were used in all experiments, with the exception of the mosaic analysis. The following *Drosophila* lines were used:

*OreR*  
*ry*<sup>506</sup>  
*y, w*  
*cyc*<sup>0</sup>, *ry*<sup>506</sup>  
*per*<sup>01</sup>; *ry*<sup>506</sup>  
*per*<sup>01</sup>; *tim*<sup>0</sup>; *ry*<sup>506</sup>  
*per*<sup>01</sup>; *cyc*<sup>0</sup>, *ry*<sup>506</sup>  
*y, w; tim*<sup>0</sup>  
*UAS-per16*  
*UAS-cyc6*  
*esg-Gal4*  
*esg-Gal4, UAS-eGFP, tub-Gal80<sup>TS</sup>*  
*myo1A-Gal4*  
*tim-Gal4*  
*hsFlp, FRT19A, tub-Gal80; act < y+ < Gal4, UAS-GFP / CyO*  
*hsFlp; act > CD2 > Gal4, UAS-nlsGFP / Cyo*  
*w; UAS-dcr2 (II)*  
*w; UAS-dcr2 (III)*  
*UAS-S/G2/M-Green / CyO*  
*cyc* RNAi (National Institute of Genetics #8727R-1, Mishima, Shizuoka, Japan)  
*per* RNAi (TRiP #JF01226, Harvard Medical School, Boston, USA).  
*Luc* RNAi (TRiP #JF01355, Harvard Medical School, Boston, USA).

Full details regarding the procedures are provided in [Extended Experimental Procedures](#).

## SUPPLEMENTAL INFORMATION

Supplemental Information includes five figures, three tables, and Extended Experimental Procedures and can be found with this article online at <http://dx.doi.org/10.1016/j.celrep.2013.03.016>.

## LICENSING INFORMATION

This is an open-access article distributed under the terms of the Creative Commons Attribution-NonCommercial-No Derivative Works License, which

permits non-commercial use, distribution, and reproduction in any medium, provided the original author and source are credited.

## ACKNOWLEDGMENTS

Stocks and antibodies were provided by Drs. Paul Hardin, Michael Rosbash, and Stephen Hou, and the Bloomington *Drosophila* Stock Center. We thank members of the Perrimon laboratory, particularly Richard Binari and Akhila Rajan, for their assistance. This work was supported by the Human Frontier Science Program (P.K.) and the Harvard Stem Cell Institute. P.E. is supported by NIH grants GM66777 and GM79182. N.P. is an investigator of the Howard Hughes Medical Institute.

Received: November 21, 2012

Revised: March 11, 2013

Accepted: March 12, 2013

Published: April 11, 2013

## REFERENCES

- Abruzzi, K.C., Rodriguez, J., Menet, J.S., Desrochers, J., Zadina, A., Luo, W., Tkachev, S., and Rosbash, M. (2011). *Drosophila* CLOCK target gene characterization: implications for circadian tissue-specific gene expression. *Genes Dev.* 25, 2374–2386.
- Akhtar, R.A., Reddy, A.B., Maywood, E.S., Clayton, J.D., King, V.M., Smith, A.G., Gant, T.W., Hastings, M.H., and Kyriacou, C.P. (2002). Circadian cycling of the mouse liver transcriptome, as revealed by cDNA microarray, is driven by the suprachiasmatic nucleus. *Curr. Biol.* 12, 540–550.
- Al-Nafussi, A.I., and Wright, N.A. (1982). Circadian rhythm in the rate of cellular proliferation and in the size of the functional compartment of mouse jejunal epithelium. *Virchows Arch. B Cell Pathol. Incl. Mol. Pathol.* 40, 71–79.
- Amcheslavsky, A., Jiang, J., and Ip, Y.T. (2009). Tissue damage-induced intestinal stem cell division in *Drosophila*. *Cell Stem Cell* 4, 49–61.
- Biteau, B., Hochmuth, C.E., and Jasper, H. (2011). Maintaining tissue homeostasis: dynamic control of somatic stem cell activity. *Cell Stem Cell* 9, 402–411.
- Borgs, L., Beukelaers, P., Vandenbosch, R., Belachew, S., Nguyen, L., and Malgrange, B. (2009). Cell “circadian” cycle: new role for mammalian core clock genes. *Cell Cycle* 8, 832–837.
- Casali, A., and Battle, E. (2009). Intestinal stem cells in mammals and *Drosophila*. *Cell Stem Cell* 4, 124–127.
- Chen, H.W., Marinissen, M.J., Oh, S.W., Chen, X., Melnick, M., Perrimon, N., Gutkind, J.S., and Hou, S.X. (2002). CKA, a novel multidomain protein, regulates the JUN N-terminal kinase signal transduction pathway in *Drosophila*. *Mol. Cell. Biol.* 22, 1792–1803.
- Fu, L., Pelicano, H., Liu, J., Huang, P., and Lee, C. (2002). The circadian gene *Period2* plays an important role in tumor suppression and DNA damage response in vivo. *Cell* 111, 41–50.
- Goulas, S., Conder, R., and Knoblich, J.A. (2012). The Par complex and integrins direct asymmetric cell division in adult intestinal stem cells. *Cell Stem Cell* 11, 529–540.
- Grima, B., Lamouroux, A., Chélot, E., Papin, C., Limbourg-Bouchon, B., and Rouyer, F. (2002). The F-box protein *slimb* controls the levels of clock proteins period and timeless. *Nature* 420, 178–182.
- Hardin, P.E. (2011). Molecular genetic analysis of circadian timekeeping in *Drosophila*. *Adv. Genet.* 74, 141–173.
- Hardin, P.E., Hall, J.C., and Rosbash, M. (1990). Feedback of the *Drosophila* period gene product on circadian cycling of its messenger RNA levels. *Nature* 343, 536–540.
- Janich, P., Pascual, G., Merlos-Suárez, A., Battle, E., Ripperger, J., Albrecht, U., Cheng, H.Y., Obrietan, K., Di Croce, L., and Benitah, S.A. (2011). The circadian molecular clock creates epidermal stem cell heterogeneity. *Nature* 480, 209–214.
- Jiang, H., Patel, P.H., Kohlmaier, A., Grenley, M.O., McEwen, D.G., and Edgar, B.A. (2009). Cytokine/Jak/Stat signaling mediates regeneration and homeostasis in the *Drosophila* midgut. *Cell* 137, 1343–1355.
- Koike, N., Yoo, S.H., Huang, H.C., Kumar, V., Lee, C., Kim, T.K., and Takahashi, J.S. (2012). Transcriptional architecture and chromatin landscape of the core circadian clock in mammals. *Science* 338, 349–354.
- Matsuo, T., Yamaguchi, S., Mitsui, S., Emi, A., Shimoda, F., and Okamura, H. (2003). Control mechanism of the circadian clock for timing of cell division in vivo. *Science* 302, 255–259.
- Medema, J.P., and Vermeulen, L. (2011). Microenvironmental regulation of stem cells in intestinal homeostasis and cancer. *Nature* 474, 318–326.
- Méndez-Ferrer, S., Lucas, D., Battista, M., and Frenette, P.S. (2008). Haematopoietic stem cell release is regulated by circadian oscillations. *Nature* 452, 442–447.
- Müller, P., Kutenkeuler, D., Gesellchen, V., Zeidler, M.P., and Boutros, M. (2005). Identification of JAK/STAT signalling components by genome-wide RNA interference. *Nature* 436, 871–875.
- Nakajima, Y., Kuranaga, E., Sugimura, K., Miyawaki, A., and Miura, M. (2011). Nonautonomous apoptosis is triggered by local cell cycle progression during epithelial replacement in *Drosophila*. *Mol. Cell. Biol.* 31, 2499–2512.
- Ni, J.Q., Liu, L.P., Binari, R., Hardy, R., Shim, H.S., Cavallaro, A., Booker, M., Pfeiffer, B.D., Markstein, M., Wang, H., et al. (2009). A *Drosophila* resource of transgenic RNAi lines for neurogenetics. *Genetics* 182, 1089–1100.
- O’Neill, J.S., and Reddy, A.B. (2011). Circadian clocks in human red blood cells. *Nature* 469, 498–503.
- Ohlstein, B., and Spradling, A. (2006). The adult *Drosophila* posterior midgut is maintained by pluripotent stem cells. *Nature* 439, 470–474.
- Pan, X., and Hussain, M.M. (2009). Clock is important for food and circadian regulation of macronutrient absorption in mice. *J. Lipid Res.* 50, 1800–1813.
- Panda, S., Antoch, M.P., Miller, B.H., Su, A.I., Schook, A.B., Straume, M., Schultz, P.G., Kay, S.A., Takahashi, J.S., and Hogenesch, J.B. (2002). Coordinated transcription of key pathways in the mouse by the circadian clock. *Cell* 109, 307–320.
- Plautz, J.D., Kaneko, M., Hall, J.C., and Kay, S.A. (1997). Independent photo-receptive circadian clocks throughout *Drosophila*. *Science* 278, 1632–1635.
- Potten, C.S., Al-Barwari, S.E., Hume, W.J., and Searle, J. (1977). Circadian rhythms of presumptive stem cells in three different epithelia of the mouse. *Cell Tissue Kinet.* 10, 557–568.
- Qiu, J.M., Roberts, S.A., and Potten, C.S. (1994). Cell migration in the small and large bowel shows a strong circadian rhythm. *Epithelial Cell Biol.* 3, 137–148.
- Sahar, S., and Sassone-Corsi, P. (2009). Metabolism and cancer: the circadian clock connection. *Nat. Rev. Cancer* 9, 886–896.
- Saito, M., Murakami, E., Nishida, T., Fujisawa, Y., and Suda, M. (1976). Circadian rhythms of digestive enzymes in the small intestine of the rat. II. Effects of fasting and refeeding. *J. Biochem.* 80, 563–568.
- Sakaue-Sawano, A., Kurokawa, H., Morimura, T., Hanyu, A., Hama, H., Osawa, H., Kashiwagi, S., Fukami, K., Miyata, T., Miyoshi, H., et al. (2008). Visualizing spatiotemporal dynamics of multicellular cell-cycle progression. *Cell* 132, 487–498.
- Scheving, L.A. (2000). Biological clocks and the digestive system. *Gastroenterology* 119, 536–549.
- Shukla, P., Gupta, D., Bisht, S.S., Pant, M.C., Bhatt, M.L., Gupta, R., Srivastava, K., Gupta, S., Dhawan, A., Mishra, D., and Negi, M.P. (2010). Circadian variation in radiation-induced intestinal mucositis in patients with cervical carcinoma. *Cancer* 116, 2031–2035.
- Stevenson, N.R., Day, S.E., and Sitren, H. (1979). Circadian rhythmicity in rat intestinal villus length and cell number. *Int. J. Chronobiol.* 6, 1–12.
- Venkei, Z., Przewłoka, M.R., and Glover, D.M. (2011). *Drosophila* Mis12 complex acts as a single functional unit essential for anaphase chromosome movement and a robust spindle assembly checkpoint. *Genetics* 187, 131–140.

Wood, P.A., Yang, X., Taber, A., Oh, E.Y., Ansell, C., Ayers, S.E., Al-Assaad, Z., Carnevale, K., Berger, F.G., Peña, M.M., and Hrushesky, W.J. (2008). Period 2 mutation accelerates *ApcMin/+* tumorigenesis. *Mol. Cancer Res.* 6, 1786–1793.

Xu, K., Zheng, X., and Sehgal, A. (2008). Regulation of feeding and metabolism by neuronal and peripheral clocks in *Drosophila*. *Cell Metab.* 8, 289–300.

Xu, K., DiAngelo, J.R., Hughes, M.E., Hogenesch, J.B., and Sehgal, A. (2011). The circadian clock interacts with metabolic physiology to influence reproductive fitness. *Cell Metab.* 13, 639–654.

Zhang, Y., Liu, Y., Bilodeau-Wentworth, D., Hardin, P.E., and Emery, P. (2010). Light and temperature control the contribution of specific DN1 neurons to *Drosophila* circadian behavior. *Curr. Biol.* 20, 600–605.

## EXTENDED EXPERIMENTAL PROCEDURES

### Housing

Animals were maintained at 25°C, 12 hr light and 12 hr dark (LD) conditions, under constant humidity. For damage, a 5% w/v sucrose (Sigma) + water solution containing either 5% w/v DSS (MP Biomedicals) or 25 ug/mL Bleocin (Calbiochem) were applied for 2 days prior to timeseries analysis (2–3 days total exposure). Chemicals were refreshed daily, and flies were maintained on LD conditions as before, with the exception of experiments where the lights were changed to complete darkness or complete light (see [Figures S1](#) and [S5](#) for experimental schematics). Female flies of < 14 days of age were used in all experiments, except in the mosaic analysis where guts were obtained from flies 23 days following clone induction.

### Dissection and Staining

Guts were dissected in 1X PBS (GIBCO) and fixed in 4% paraformaldehyde (Electron Microscopy Sciences) diluted with 1X PBS. Samples were washed 3X with PBS, then blocked for 30 min in 1X PBS, 1% BSA (Sigma), 0.2% Triton X-100 (Sigma). The following antibodies were used: Rabbit anti-Period, Mouse anti-Delta (Developmental Studies Hybridoma Bank), Mouse anti-Prospero (Developmental Studies Hybridoma Bank), Mouse anti-Fibrillarin (Encore Biotechnology), Rabbit anti-phospho-Histone3 (Millipore). Samples were washed 3X with PBS, and stained with secondary antibodies: Donkey anti-mouse Alexa 555 (Molecular Probes), Donkey anti-mouse Alexa 647 (Molecular Probes), Goat anti-rabbit Alexa 488 (Molecular Probes), Donkey anti-rabbit Alexa 555 (Molecular Probes). EdU exposure was carried out for 45 min on dissected guts according to the manufacturer's instructions, labeling was also performed according to the Click-iT EdU Alexa Fluor 555 Imaging Kit (Invitrogen) instructions. All samples were counterstained with DAPI (Molecular Probes) and mounted using Vectashield (Vector). For brain dissection, 2–5 day post-eclosion flies were entrained 3 days under LD conditions, and were stained as described in Zhang et al. ([Zhang et al., 2010](#)).

### RNAi Screen

We performed a genetic screen for transcription factors required in *Drosophila* ISCs during regeneration, by expressing *UAS-RNAi* constructs ([Ni et al., 2009](#)) to suppress transcription factors/regulators, using a temperature-inducible *esg-Gal4*, *tub-Gal80TS* driver. Flies were raised at 18°C to prevent the expression of *UAS-RNAi*, then, at 2–5 days post-eclosion, shifted to 29°C for 8 days to induce expression in ISCs. Flies were exposed to 5% DSS for an additional 3 days, and guts were dissected and stained for phospho-Histone3 as described above. Total mitoses per gut were scored for each RNAi and compared to *Luc* RNAi controls, whose division is increased 10–20 fold from baseline in the presence of DSS. Two separate RNAi constructs for *per* were recovered as strong hits in the screen, suppressing division by at least 80%.

### RNA Purification and qRT-PCR

15–20 midguts from each genotype were collected in RNAlater reagent (QIAGEN; n = 3 biological replicates). mRNA was isolated using a Oligotex Direct mRNA Mini Kit and/or RNA using the RNEasy Mini Kit (QIAGEN), and the iScript cDNA Synthesis Kit (Biorad) was used to transcribe cDNA. qPCR was then carried out on a CFX96 Real-Time System / C1000 Thermal Cycler (Biorad) with iQ SYBR Green Supermix (Biorad). Expression was normalized to *GAPDH* control transcript, then normalized relative to the appropriate control at ZT15. qPCR primers:

```
GAPDH1-F: CCAATGTCTCCGTTGTGGA
GAPDH1-R: TCGGTGTAGCCCAGGATT
per-F: TCATCCAGAACGGTTGCTACG
per-R: CCTGAAAGACGCGATGGTGT
tim-F: CCAGCATTCAATCCAAGCAG
tim-R: GCGTGGCAAACACTGTGTATG
Cka-F: aaggatgctcaccgagga
Cka-R: gccatcagattcgattacc
Kmn1-F: tcgctatgaagcaagcacttt
Kmn1-R: cctcgtcctcctgacagcta
lpk2-F: attgccgcttcagaggt
lpk2-R: atgacggcgcggttagtagt
```

### Microarray Analysis

n = 20 midguts, in duplicate, were collected every 4h over 24h following Bleocin damage. RNA was purified as above, then processed and hybridized on Affymetrix *Drosophila* Genome 2.0 chips, according to the manufacturer's instructions, at the Microarray Core, Dana-Farber Cancer Institute. Data were normalized and analyzed as described in [Xu et al. \(2011\)](#).

### Survival Assays

Flies were maintained under light/dark conditions as above. Flies were fed either 5% or 10% w/v DSS (MP Biomedicals) or 25 ug/mL Bleocin (Calbiochem), mixed in a solution of 5% w/v sucrose (Sigma). Approximately 15 flies were loaded per vial ( $n = 3$  vials per genotype), and solutions were refreshed daily. Survival was scored each day and assays were performed on 2 separate occasions.

### CAFÉ and Blue-Dye Assays

Flies were maintained under light/dark conditions as above. Blue dye assay was performed as reported in Xu et al. (2008) For the CAFÉ assay, 5 mL of 1% *Drosophila* Type II Agar (Apex BioResearch Products) was solidified in one vial to provide hydration. 5-10 flies were loaded into each of these vials and a capillary of feeding solution (5% w/v sucrose and 2.5% w/v yeast extract) was presented in each. Flies were maintained for one day, to acclimatize to feeding from capillaries, before the start of the assay. Capillaries were refreshed once every 3 hr, and the solution levels consumed in each capillary noted.

### Behavior Assay

Adult flies (2–5 days old) were entrained for 3 days under LD (500 lux intensity), and then released into constant darkness for at least 5 days. Single fly locomotor activity was measured with TriKinetics Activity Monitors (Waltham, MA) in I36-LL Percival Incubators. Data analysis was performed using the FAAS-X software (Grima et al., 2002).

### Mosaic Analysis

Flies were maintained on a 12–12 light/dark cycle, as above, and transferred to fresh media every 1–2 days. For MARCM clones two 1 hr 37°C heat shocks were applied at 2–3 days following eclosion, while for RNAi clones one 12 min 37°C heat shock was applied at 2–3 days following eclosion. A region of leaky GFP expression was noted in the RNAi clone stock, and this was omitted from these analyses. Clones were scored as clusters of 2 or more directly adjacent cells.

### Imaging and Data analysis

Confocal microscopy was done using the Zeiss LSM 780 with the Zen LSM software package (Zeiss). Images were processed in Photoshop CS5.1 (Adobe). The percentage of cells was calculated by determining the number of (+) cells of interest divided by the total DAPI+ nuclei in one FOV from posterior midgut using a 40X objective. ~300–400 cells were scored per FOV per midgut, and > 5 midguts were analyzed per genotype. The same approach was used to quantify the percentage of (+) cells using the FUCI cell cycle reporter and EdU, but in these cases, the total was that of the total DI+ or total diploid cell nuclei present, respectively. Statistics (either paired or unpaired t tests, or ANOVA with Dunnett's post-test to compare to controls, as appropriate) were carried out using Graphpad Prism 5.0.

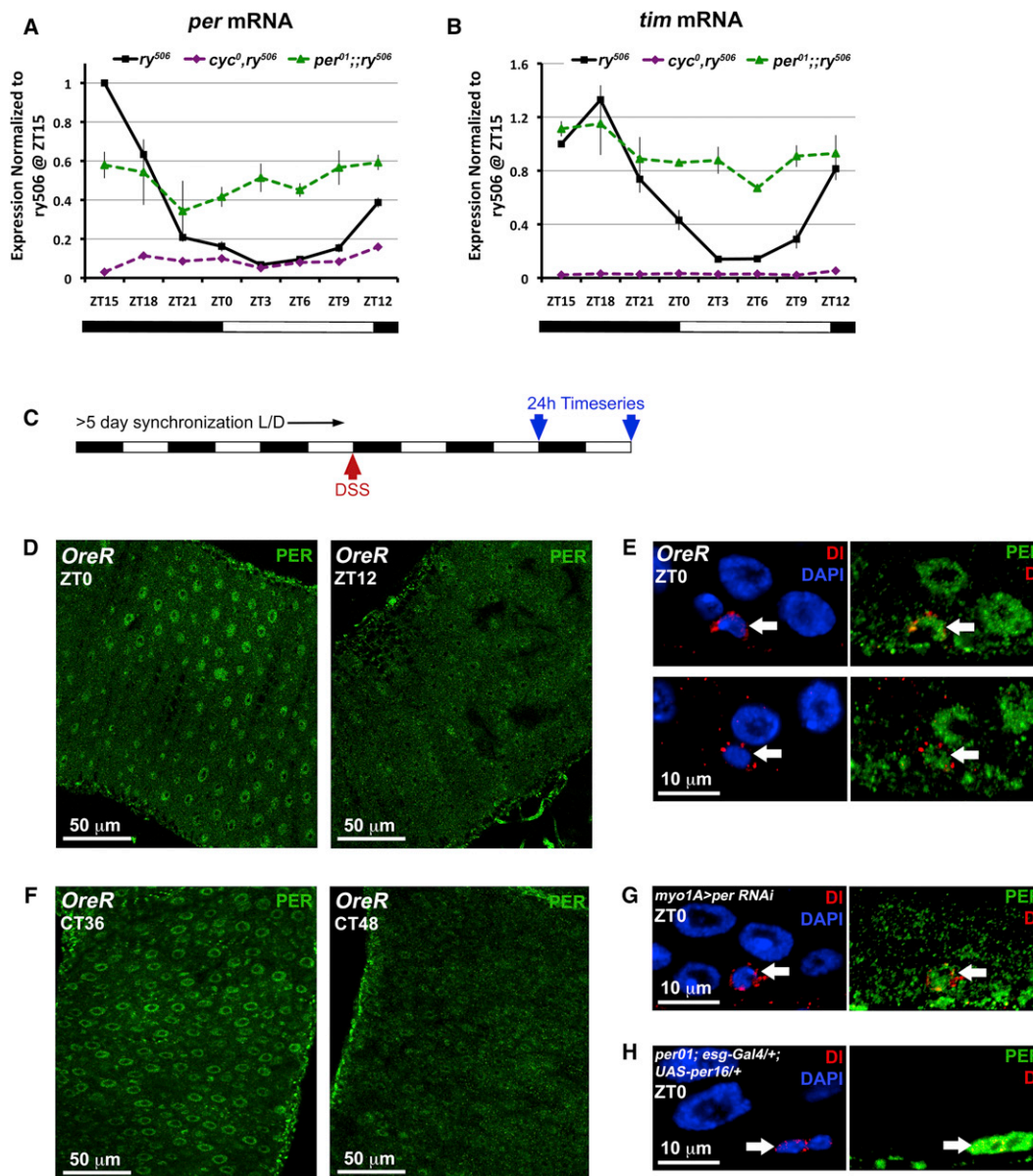


**Figure S1. PER/TIM Expression in the Gut, Related to Figures 1 and 2**

(A) *per* RNA expression (qPCR) over Zeitgeber Time (ZT) normally shows circadian rhythms in the intestine ( $ry^{506}$  control), which are absent in  $per^{01}$  ( $ry^{506}$  and  $per^{01}$  data are the same as in Figure 1B). The  $per^{01}$  mutation is a nonsense mutation at exon 4 that produces a truncated non-functional product. *per* expression is very low in  $cyc^0$ , because *per* is a direct transcriptional target of CLK/CYC.

(B) *tim* is also a clock target and fluctuates in the same manner as *per*. *tim* RNA remains high in the  $per^{01}$  mutant (qPCR), and the  $cyc^0$  mutant shows very low *tim* RNA level. As *per/tim* are transcribed by CLK/CYC they increase in level and eventually repress their own transcription. Degradation of PER/TIM eventually frees CLK/CYC, thus completing the feedback loop. Graphs a-b show average of 2 separate experiments ( $n = 15$  guts/genotype/time point,  $p < 0.05$  by ANOVA, expression normalized to  $ry^{506}$  ZT15, relative to *GAPDH* control RNA, error bars  $\pm$  SEM).

(C) Schematic shows synchronization of flies on 12-12 LD cycle (for at least 3 days), followed by DSS (or Bleocin) application and 24 hr analysis 2 days later. See [Extended Experimental Procedures](#) for full description.

(D) PER staining (green) shows nuclear accumulation in intestinal epithelial cells in the morning (ZT0) versus the evening (ZT12), ECs can be recognized by their large polyploid nuclei.

(E) At ZT0, PER protein is expressed in ISCs (arrows) labeled with Delta (DI, red).

(F) PER staining under DD conditions similarly shows accumulation and reduction over 24h rhythms.

(G) PER protein does not accumulate in ECs at ZT0 when *per RNAi* is expressed in ECs using *myo1A-Gal4*.

(H) Similarly PER is not present in ECs, but is present in ISCs and EBs when the PER rescue construct is forcibly expressed using *esg-Gal4* in the  $per^{01}$  mutant background. Note that PER is present at much higher levels using the rescue construct (compare with Figure 1D and S1E). This suggests the ISCs and ECs are desynchronized in these two experiments.

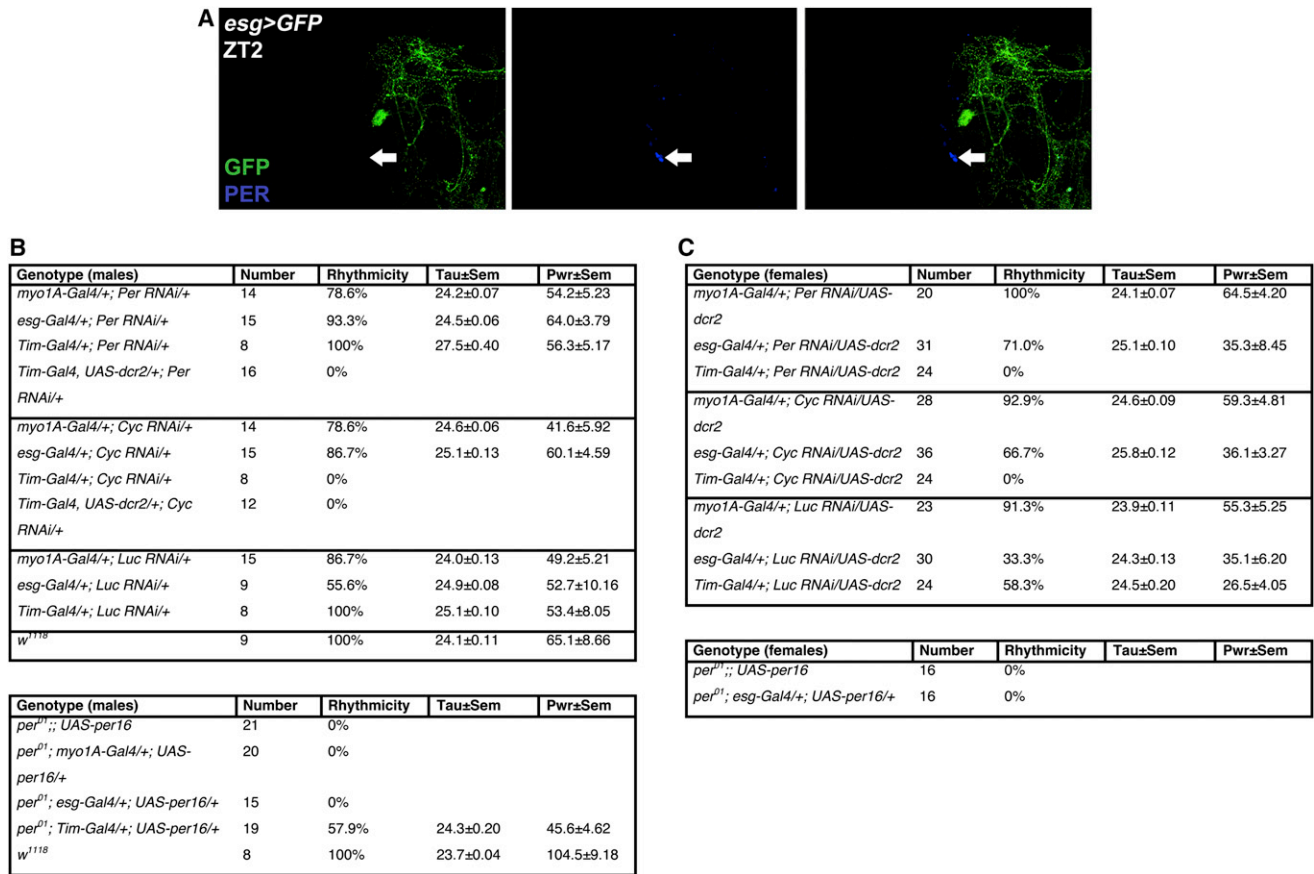


**Figure S2. Validation of RNAi and Rescue Reagents, Related to Figures 1, 2, 3, and 4**

(A) The *esg-Gal4* driver (*esg > GFP* is *esg-Gal4, UAS-GFP*) is expressed in several neurons in the brain, but it is not expressed in pacemaker neurons stained for PER protein (blue). Image shows a single confocal plane. Similarly, *myo1A-Gal4* was not colocalized with pacemaker neurons (not shown).

(B and C) Tables show periods of activity in male and female flies in constant darkness, following light/dark synchronization. Flies normally exhibit characteristic peaks of activity in the early morning and late evening which oscillate in a circadian manner (see for instance *w<sup>1118</sup>* and *Luc RNAi* controls). Expression of *UAS-per RNAi* in pacemaker neurons using *tim-Gal4* completely disrupts behavior rhythms with *UAS-dcr2*, and increases the period of rhythms without *UAS-dcr2*. Similarly, *UAS-cyc RNAi* in pacemaker neurons completely disrupts behavior rhythms with and without *UAS-dcr2*. In contrast behavior rhythms persist when the same constructs are expressed in ISCs using *esg-Gal4*, or in ECs using *myo1A-Gal4*. We note, however, that the period of behavior rhythms is slightly (~1h) longer than 24h in *esg > Luc RNAi* (24.9h for males, 24.3 for females), *esg > cyc RNAi* (25.1 for males, 25.8 for females), and *esg > per RNAi* (24.5h for males, 25.1 for females). We further tested the possibility that the *esg-Gal4* and *myo1A-Gal4* drivers were expressed in the brain, by using them to express a rescue construct, *UAS-per16*, in the *per<sup>01</sup>* mutant background. *per<sup>01</sup>* flies are completely arrhythmic, but *tim-Gal4* driven expression of *UAS-per16* effectively restores behavior rhythms. In contrast, neither *esg-Gal4* or *myo1A-Gal4* restore rhythms to *per<sup>01</sup>*. The *tubulin-Gal4* driver knocks down *cyc* mRNA (*tub-Gal4/+;UAS-cyc RNAi/+*) to 20% of wild-type *cyc* levels at ZT3, and *per* mRNA (*tub-Gal4/+;UAS-per RNAi/+*) to 25% of wild-type *per* levels at ZT15 (peak of *per* expression). These data support the use of the *esg-Gal4* and *myo1A-Gal4* drivers and RNAi constructs to disrupt circadian rhythms in ISCs or ECs, respectively, without affecting circadian behavior.

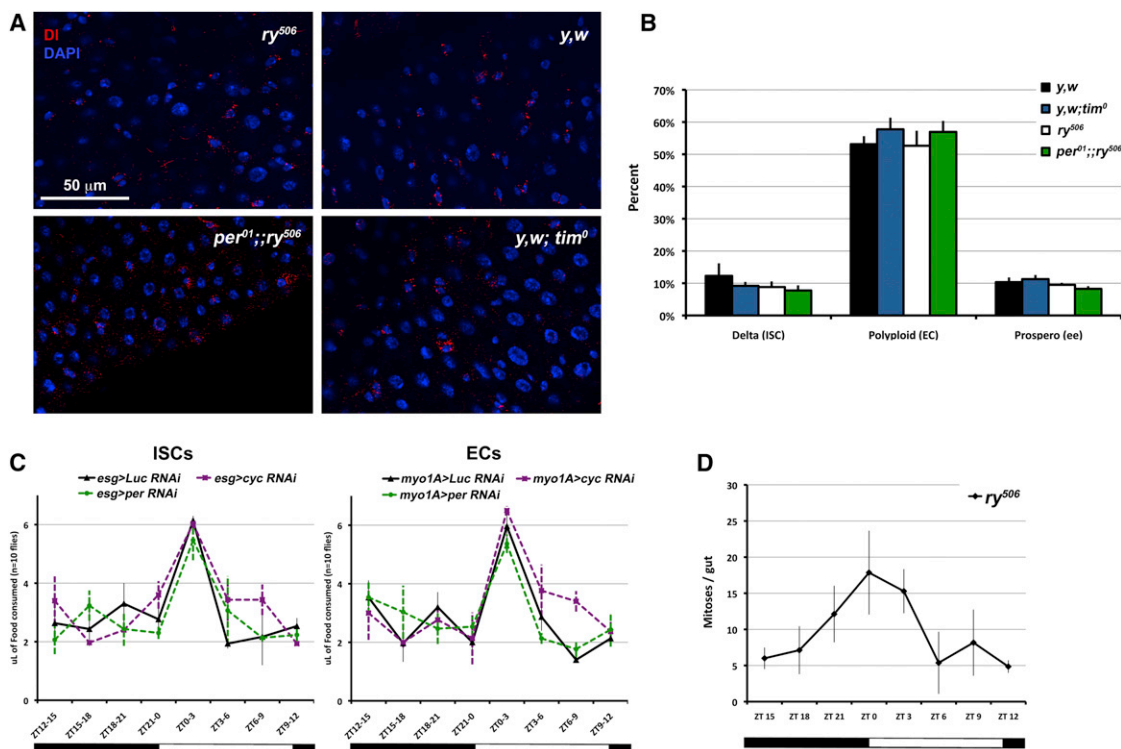


**Figure S3. Circadian Clock Mutants Show No Obvious Intestinal Cell Deficiencies, and Rhythmic Mitoses in the Intestine Are Not Dependent on Feeding, Related to Figures 1, 2, 3, and 4**

(A) ISCs, labeled for Delta (DI, red) are evident in both *per<sup>01</sup>* and *tim<sup>0</sup>* mutant intestines.

(B) The proportion of ISCs (%Delta+), ECs (%polyploid nuclei), or ees (%Prospero+) does not significantly vary between *per<sup>01</sup>* and *tim<sup>0</sup>* mutant, and *ry<sup>506</sup>* or *y,w* control intestines. *cyc<sup>0</sup>* mutant intestines showed a similar proportion of these cell types (not shown).

(C) If perturbation of circadian rhythms affected feeding, the reduction and arrhythmic intestinal mitoses in the *per<sup>01</sup>* mutant or the *esg > per RNAi* could be simply a result of insufficient uptake of DSS. It has been previously shown that circadian clock genes regulate the timing of feeding rhythms, but that mutants do not feed less over a 24h period (Xu et al., 2008). Although we did not observe any mitotic rhythms in the intestine of the mutants tested, the CAFÉ assay, was applied to test the amount of food consumed by flies over 24 hr. The volume of media consumed was measured at 3h intervals, where knockdown of CYC or PER in either the ISCs or ECs had no effect on feeding. Because mitoses peak at ZT0, and the highest level of food consumed is from ZT0-ZT3, this suggests that mitoses peak before feeding levels. In addition, the amount of food consumed over the entire 24h period was equivalent between all of these genotypes (not shown). For instance, *esg > per RNAi* shows very low and arrhythmic mitoses at all time points (Figure 1F), but feeds equivalently to the *esg > Luc RNAi* control, whose mitoses are higher and rhythmic over the same time points. Finally, we tested feeding levels using a blue-dye uptake assay and found that *ry<sup>506</sup>*, *per<sup>01</sup>*, *cyc<sup>0</sup>* and *tim<sup>0</sup>* animals fed equivalently over 24 hr (not shown).

(D) Flies were entrained on LD conditions as before but food was presented from ZT12-ZT0 only, and flies were shifted onto 5% agar/H<sub>2</sub>O from ZT0-ZT12. Following 2 days DSS exposure (ZT12-ZT0 only), mitotic rhythms still peak at ZT0 further suggesting that ISC division is independent from the timing of DSS consumption. We note, however, that mitoses are reduced in these conditions, perhaps as a result of the restricted availability of DSS.

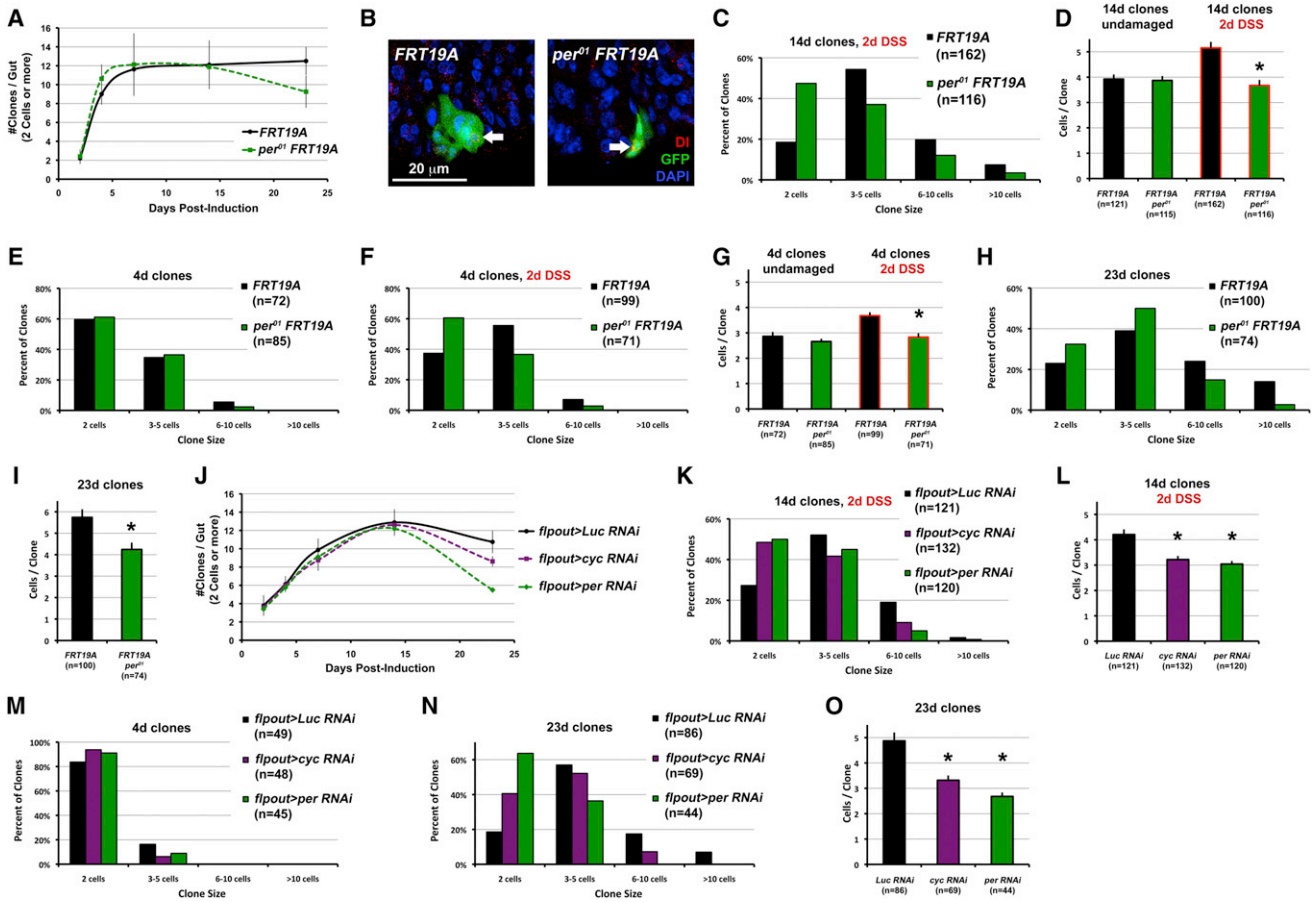


**Figure S4. ISC-Autonomous Proliferation Is Decreased when CYC or PER Is Lost, Related to Results and Discussion**

(A) The frequency of proliferating clones ( $\geq 2$  cells in size) in the whole gut was measured over 23 days following clonal induction ( $n = 10$  guts/genotype/time point, error bars  $\pm$  SEM).

(B and C) 14 days following induction, control (*FRT19A* is *FRT19A/hsFlp,FRT19A, Tub-Gal80; act > y+ > Gal4, UAS-GFP/+*) clones, under 2 days DSS damage, are larger than *per* mutant clones (*per<sup>01</sup> FRT19A* is *per<sup>01</sup>, FRT19A/hsFlp,FRT19A, Tub-Gal80; act > y+ > Gal4, UAS-GFP/+*). Note that DI+ cells are present in *per<sup>01</sup>* clones, indicating that the ISCs are not lost. *per<sup>01</sup>* clones show a different distribution of sizes, brackets indicate number of clones examined.

(D) 14 days following induction, *per<sup>01</sup>* are the same size as wild-type, however upon damage *per<sup>01</sup>* clones are slightly but significantly smaller. Damaged clones are same as those reported in Figure S4C. Brackets indicate number of clones examined, \*significance by t test ( $p < 0.05$ ).

(E) At 4 days, the size of *per<sup>01</sup>* clones is similar to controls. Brackets indicate number clones examined.

(F) 4 day *per<sup>01</sup>* clones, exposed to DSS for 2 days, show a different distribution of sizes. Brackets indicate number of clones examined.

(G) 4 days following induction, *per<sup>01</sup>* are the same as wild-type, however upon damage *per<sup>01</sup>* clones are slightly but significantly smaller. Damaged clones are the same as those reported in Figure S4F. Brackets indicate number of clones examined, \*significance by t test ( $p < 0.05$ ).

(H) At 23 days, in the absence of damage, *per<sup>01</sup>* clones show a different distribution of sizes. Brackets indicate number of clones examined.

(I) The average size of *per<sup>01</sup>* clones at 23 days following induction, even in the absence of damage, is significantly smaller than controls. Clones are the same as those in Figure S4H. Brackets indicate number of clones examined, \*significance by t test ( $p < 0.05$ ).

(J) The same assay was undertaken using RNAi clones (for instance the control *flpout > Luc RNAi* refers to *hsFlp/+; act > CD2 > Gal4, UAS-nlsGFP/UAS-dcr2; UAS-Luciferase RNAi/+*). All genotypes are only different in the RNAi transgene on chromosome 3 ( $n = 10$  guts/genotype/time point, error bars  $\pm$  SEM).

(K) 14 day *cyc RNAi* and *per RNAi* clones, exposed to DSS for 2 days, show a different distribution of sizes. Brackets indicate number of clones examined.

(L) *cyc RNAi* and *per RNAi* clones are slightly but significantly smaller. Clones are the same as those reported in Figure S4K. Brackets indicate number of clones examined, \*significance by t test ( $p < 0.05$ ).

(M) At 4 days, the size of *cyc RNAi* and *per RNAi* clones is similar to controls. Brackets indicate number clones examined.

(N) At 23 days, with no damage, both *cyc RNAi* and *per RNAi* clones show different size distributions compared to *Luc RNAi* controls. Brackets indicate number clones examined.

(O) Both *cyc RNAi* and *per RNAi* 23 day clones are slightly but significantly smaller. Clones are the same as those reported in Figure S4N. Brackets indicate number of clones examined, \*significance by t test ( $p < 0.05$ ).

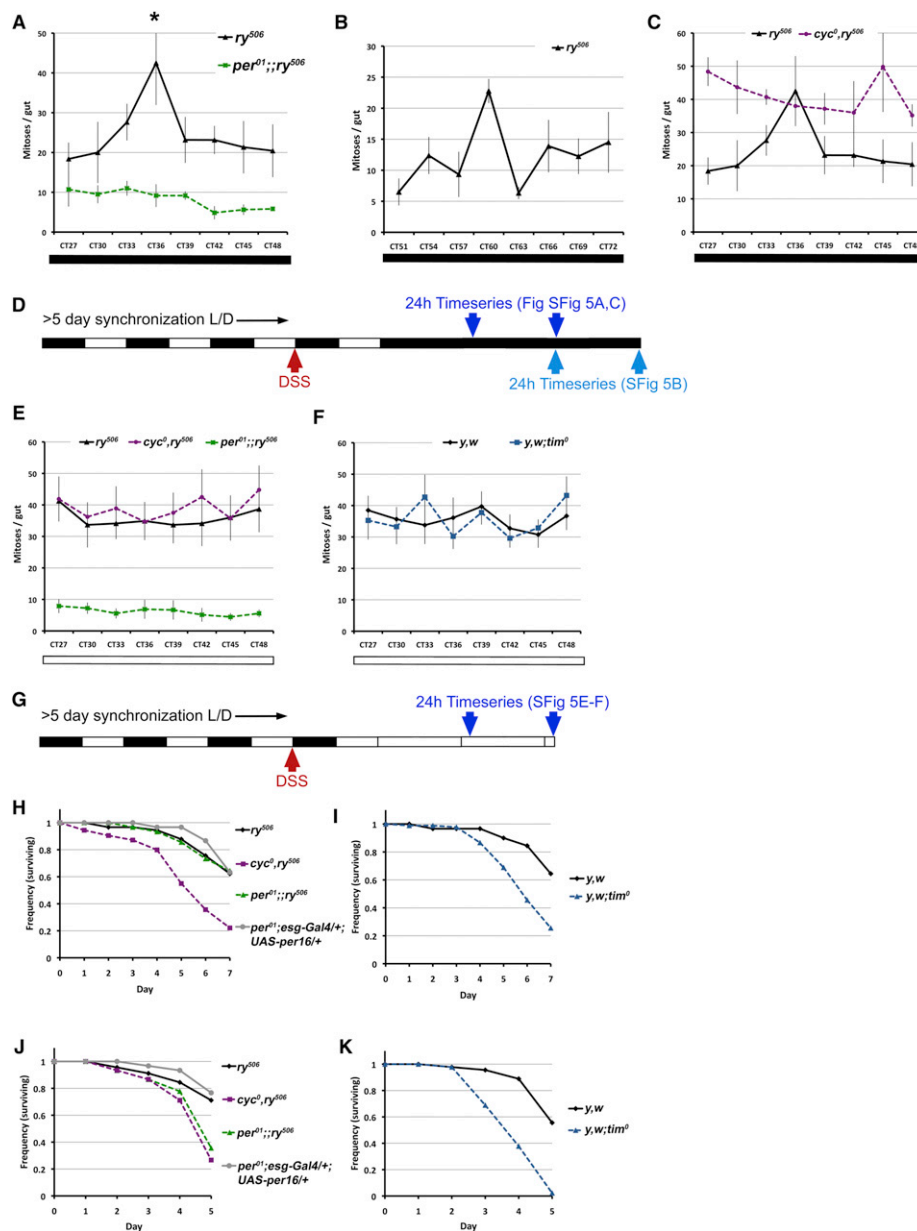


**Figure S5. Mitotic Rhythms Are True Circadian Rhythms and Are Required for Survival following Gut Damage, Related to Figures 1, 2, and 4**

(A) If lights are turned off, after light/dark synchronization (see schematic below), rhythms in mitoses persist 2 days later in  $ry^{506}$  but not in  $per^{O1}$ .  
 (B) If lights are turned off, after light/dark synchronization, rhythms in mitoses also persist 3 days later in  $ry^{506}$ . The peak in mitoses seen at 2–3 days DD thus repeats itself 24h later, at 3–4 days, in the absence of light cues.  
 (C)  $cyc^O$  mutant intestines were examined when flies were shifted from 12–12 light/dark conditions to complete darkness (as in schematic below). The circadian rhythms in controls are perpetuated in these conditions ( $ry^{506}$  data is taken from Figure S5A), but  $cyc^O$  intestines remain arrhythmic and at same levels as in Figure 2A. Graphs show  $n = 10$  guts/genotype/time point (error bars  $\pm$  SEM).  
 (D) Schematic shows synchronization of flies on 12–12 Light/Dark cycle (for at least 3 days), followed by DSS application, shifting to complete darkness, and 24 hr analysis 2 days later. See [Extended Experimental Procedures](#) for full description.  
 (E and F) When light/dark synchronized flies are exposed to constant light (as in schematic below), mitotic rhythms in the intestine are no longer observed ( $n = 10$  guts/genotype/time point, error bars  $\pm$  SEM). Neither  $ry^{506}$  nor  $y,w$  control flies exhibit peaks of mitoses at ZTO under constant light (compare with Figures 1E, 2A, and 2B), rather these show high mitoses at all times.  
 (G) Schematic shows synchronization of flies on 12–12 Light/Dark cycle (for at least 3 days), followed by DSS application, shifting to complete light, and 24 hr analysis 2 days later. See [Extended Experimental Procedures](#) for full description.  
 (H and I) Survival of circadian mutant animals compared to their respective controls on 5% DSS (black lines).  $cyc^O$  and  $tim^O$  mutants show reduced survival on 5% DSS.  
 (J and K) Survival assays of same genotypes on 10% DSS, where  $cyc^O$ ,  $tim^O$ , and  $per^{O1}$  mutants show reduced survival as they do on Bleocin (Figures 2H and 2I) Graphs show representative experiments ( $n = 3$  vials/15 flies per vial, genotypes are as above).